



Protection Against Malaria by Intravenous Immunization with a Nonreplicating Sporozoite Vaccine

Robert A. Seder *et al.*
Science **341**, 1359 (2013);
DOI: 10.1126/science.1241800

This copy is for your personal, non-commercial use only.

If you wish to distribute this article to others, you can order high-quality copies for your colleagues, clients, or customers by [clicking here](#).

Permission to republish or repurpose articles or portions of articles can be obtained by following the guidelines [here](#).

The following resources related to this article are available online at www.sciencemag.org (this information is current as of September 23, 2013):

Updated information and services, including high-resolution figures, can be found in the online version of this article at:

<http://www.sciencemag.org/content/341/6152/1359.full.html>

Supporting Online Material can be found at:

<http://www.sciencemag.org/content/suppl/2013/08/07/science.1241800.DC1.html>

<http://www.sciencemag.org/content/suppl/2013/08/07/science.1241800.DC2.html>

A list of selected additional articles on the Science Web sites **related to this article** can be found at:

<http://www.sciencemag.org/content/341/6152/1359.full.html#related>

This article **cites 46 articles**, 22 of which can be accessed free:

<http://www.sciencemag.org/content/341/6152/1359.full.html#ref-list-1>

This article has been **cited by 1** articles hosted by HighWire Press; see:

<http://www.sciencemag.org/content/341/6152/1359.full.html#related-urls>

Protection Against Malaria by Intravenous Immunization with a Nonreplicating Sporozoite Vaccine

Robert A. Seder,^{1*†} Lee-Jah Chang,^{1*} Mary E. Enama,¹ Kathryn L. Zephir,¹ Uzma N. Sarwar,¹ Ingelise J. Gordon,¹ LaSonji A. Holman,¹ Eric R. James,² Peter F. Billingsley,² Anusha Gunasekera,² Adam Richman,² Sumana Chakravarty,² Anita Manoj,² Soundarapandian Velmurugan,² MingLin Li,³ Adam J. Ruben,² Tao Li,² Abraham G. Eappen,² Richard E. Stafford,^{2,3} Sarah H. Plummer,¹ Cynthia S. Hendel,¹ Laura Novik,¹ Pamela J. M. Costner,¹ Floreliz H. Mendoza,¹ Jamie G. Saunders,¹ Martha C. Nason,⁴ Jason H. Richardson,⁵ Jittawadee Murphy,⁵ Silas A. Davidson,⁵ Thomas L. Richie,⁶ Martha Sedegah,⁶ Awalludin Sutamihardja,⁶ Gary A. Fahle,⁷ Kirsten E. Lyke,⁸ Matthew B. Laurens,^{8,9} Mario Roederer,¹ Kavita Tewari,¹ Judith E. Epstein,⁶ B. Kim Lee Sim,^{2,3} Julie E. Ledgerwood,¹ Barney S. Graham,^{1‡} Stephen L. Hoffman,^{2,3‡} the VRC 312 Study Team[§]

Consistent, high-level, vaccine-induced protection against human malaria has only been achieved by inoculation of *Plasmodium falciparum* (Pf) sporozoites (SPZ) by mosquito bites. We report that the PfSPZ Vaccine—composed of attenuated, aseptic, purified, cryopreserved PfSPZ—was safe and well tolerated when administered four to six times intravenously (IV) to 40 adults. Zero of six subjects receiving five doses and three of nine subjects receiving four doses of 1.35×10^5 PfSPZ Vaccine and five of six nonvaccinated controls developed malaria after controlled human malaria infection ($P = 0.015$ in the five-dose group and $P = 0.028$ for overall, both versus controls). PfSPZ-specific antibody and T cell responses were dose-dependent. These data indicate that there is a dose-dependent immunological threshold for establishing high-level protection against malaria that can be achieved with IV administration of a vaccine that is safe and meets regulatory standards.

Malaria control interventions, including insecticide-impregnated bednets, insecticide spraying, and antimalarial drugs, have substantially reduced malaria morbidity and mortality (1). However, despite these measures there were in 2010 an estimated 220 million clinical cases and 0.66 to 1.24 million deaths caused by malaria (1, 2). A highly effective vaccine will be ideal for preventing malaria in individuals and eliminating malaria in defined geographic areas. It would optimally target the parasite at asymptomatic, pre-erythrocytic stages

(3, 4). The World Health Organization malaria vaccine technology roadmap set a vaccine efficacy goal of 80% by 2025 (5). Heretofore, no injectable malaria vaccine candidate has consistently approached that level of efficacy.

RTS,S/AS01 is the most advanced subunit malaria vaccine, protecting ~50% of subjects against controlled human malaria infection (CHMI) 2 to 3 weeks after the last dose of vaccine and 22% at 5 months after last immunization (6). In a large-scale phase 3 efficacy trial in African infants 6 to 12 weeks of age, RTS,S/AS01 reduced the rates of clinical and severe malaria acquired over a 12-month period by 31.3 and 36.6%, respectively (7).

It has been known for 40 years that it is possible to achieve high-level, sustained, protective immunity against the pre-erythrocytic stages of the parasite through immunization by the bites of >1000 irradiated mosquitoes carrying *Plasmodium falciparum* (Pf) sporozoites (SPZ) (8–11). Advancing this technique beyond administration by mosquitoes required the capacity to manufacture aseptic, radiation-attenuated, metabolically active, purified, cryopreserved PfSPZ for an injectable vaccine that met regulatory standards (12). This was achieved (13, 14), and the first clinical trial of the PfSPZ Vaccine, composed of Pf NF54 strain SPZ (15), was conducted in 80 adults (14), who received up to 6 doses of 1.35×10^5 PfSPZ

Vaccine subcutaneously (SC) or intradermally (ID). The PfSPZ Vaccine was safe and well-tolerated but elicited low-level immune responses and minimal protection. We hypothesized that the limited efficacy was due to the inefficiency of ID and SC administration for sufficient presentation of PfSPZ antigens at critical inductive sites required to achieve a protective immunological threshold (16). Therefore, we immunized nonhuman primates (NHPs) with the PfSPZ Vaccine and showed that intravenous (IV), but not SC, administration of the PfSPZ Vaccine elicited potent and durable PfSPZ-specific T cell responses in peripheral blood and most notably in the liver (14), the likely site of immune protection (17). On the basis of these data, we hypothesized that IV administration of the PfSPZ Vaccine would be protective in humans (14) and conducted a phase 1 clinical trial in order to determine safety, immunogenicity, and protective efficacy against CHMI of IV immunization with the PfSPZ Vaccine (18).

Study Population

Fifty-seven subjects, composed of 40 vaccine recipients, 12 CHMI controls, and five back-up controls, enrolled from October 2011 to October 2012 (baseline characteristics are shown in table S1). Thirty-six of 40 (90%) subjects completed all scheduled vaccinations (Fig. 1 and fig. S1). Of these 36 subjects, two were immunized with 2×10^3 PfSPZ Vaccine per dose so as to assess safety only on schedules without CHMI, whereas at higher doses, CHMI was administered to 17 in July 2012 and to 15 in October 2012. Two subjects in the 1.35×10^5 PfSPZ Vaccine-per-dose group did not undergo CHMI because of an unrelated serious adverse event (SAE) and travel, respectively (Fig. 1).

Adverse Events

Vaccinations were well tolerated, and there were no breakthrough malaria infections before CHMI (Table 1). Thirty (75%) vaccine recipients had no local reactogenicity, nine (22.5%) had mild pain and tenderness or bruising, and one (2.5%) had moderate bruising at the injection site (Table 1 and table S2). Solicited systemic reactogenicity was none for 19 (47.5%), mild for 16 (40%), moderate for four (10%) and severe for one (2.5%) subject (Table 1 and table S3); the latter reported a headache after the third dose of 1.35×10^5 PfSPZ Vaccine.

Transient, asymptomatic increases in aspartate aminotransferase (AST) and/or alanine aminotransferase (ALT), assessed as possibly related to vaccination, were observed in 16 (40%) of vaccinees and were not dose-dependent (table S4 and figs. S2 and S3). Two SAEs occurred: One subject was diagnosed with colon cancer and did not participate in CHMI. After CHMI, one vaccine recipient developed anxiety and headache 14 days after completing chloroquine treatment and was hospitalized overnight for diagnostic

¹Vaccine Research Center (VRC), National Institute of Allergy and Infectious Diseases, National Institutes of Health, Bethesda, MD 20852, USA. ²Sanaria, Rockville, MD 20850, USA. ³Protein Potential, Rockville, MD 20850, USA. ⁴Biostatistics Research Branch, Division of Clinical Research, National Institute of Allergy and Infectious Diseases, National Institutes of Health, Bethesda, MD 20852, USA. ⁵Entomology Branch, Walter Reed Army Institute of Research, Silver Spring, MD 20910, USA. ⁶U.S. Military Malaria Vaccine Program, Naval Medical Research Center, Silver Spring, MD 20910, USA. ⁷Department of Laboratory Medicine, National Institutes of Health, Bethesda, MD 20892, USA. ⁸Center for Vaccine Development, University of Maryland School of Medicine, Baltimore, MD 21201, USA. ⁹Howard Hughes Medical Institute, Baltimore, MD 21201, USA.

*These authors contributed equally to this work.

†To whom correspondence should be sent. E-mail: rseder@mail.nih.gov

‡These authors contributed equally to this work.

§The VRC 312 Study Team members are listed in the supplementary materials.

purposes. The symptoms, which were attributed to chloroquine, resolved within 1 month.

Vaccine Efficacy CHMI #1

In July 2012, subjects who received 7.5×10^3 and 3×10^4 PfSPZ Vaccine per dose underwent CHMI ~3 weeks after last immunization, and 16 of 17 developed parasitemia (Fig. 2). Among the nine subjects who had received four doses of 3×10^4 PfSPZ Vaccine, one did not develop parasitemia, whereas the other eight had a 1.4-day prolongation of time to parasitemia by thick blood smear (prepatent period) as compared with the six nonvaccinated controls ($P = 0.007$, Log-Rank) (Fig. 2 and table S5). This observation suggests a modest reduction in the numbers of liver stage parasites. The prepatent periods in the 7.5×10^3 PfSPZ Vaccine-per-dose group were

not significantly different than those of controls (Fig. 2 and table S5).

Second Vaccine Efficacy CHMI

In October 2012, subjects who received 1.35×10^5 PfSPZ Vaccine per dose underwent CHMI ~3 weeks after last immunization along with six new controls. Five of six controls developed parasitemia. Three of nine subjects in the four-dose group and none of six in the five-dose group developed parasitemia ($P = 0.015$ for the five-dose group versus controls, Fisher's exact test) (Fig. 2 and table S5). All subjects who did not develop parasitemia detected with thick blood smear were negative as determined by means of quantitative polymerase chain reaction (PCR) at 28 days after CHMI. In the three vaccinated subjects that became infected, there was a modest

delay in the time to positive PCR (table S5). Overall, 12 of 15 subjects immunized with 1.35×10^5 PfSPZ Vaccine per dose were protected ($P = 0.028$) (Fig. 2 and table S5).

Antibody Responses

Monoclonal antibodies against the major surface protein on SPZ, the circumsporozoite protein (CSP), prevent malaria by blocking SPZ invasion and development in hepatocytes (19). Furthermore, the RTS,S/AS01 malaria vaccine is thought to mediate protection primarily through the induction of high levels of antibodies against PfcSP (20). Antibodies mediate some protection in rodents immunized with irradiated SPZ (21). In human subjects immunized via irradiated PfSPZ-infected mosquito bites, PfcSP or PfSPZ antibody titers have been detected by means of enzyme-

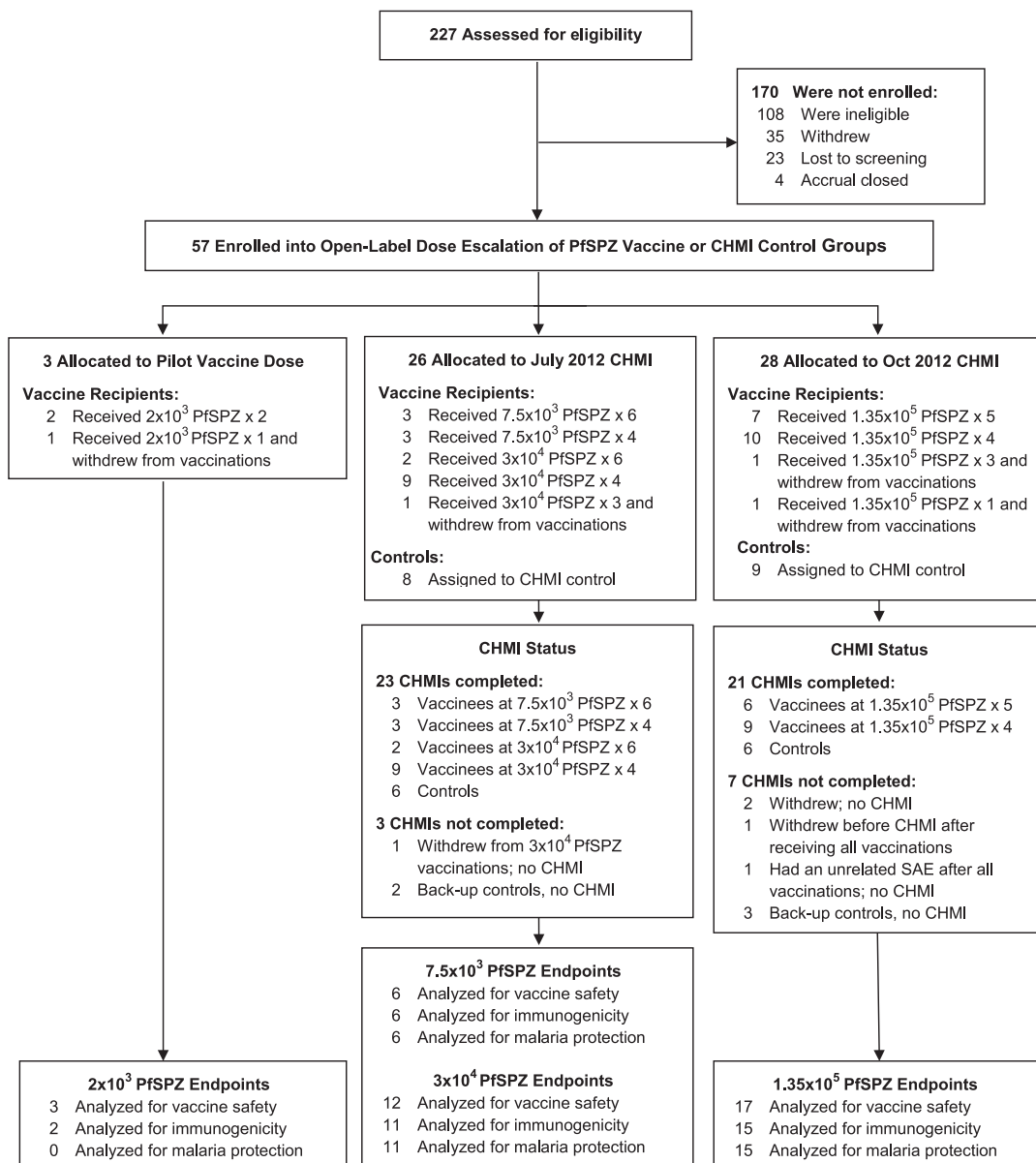


Fig. 1. Screening, enrollment, vaccinations, CHMI, and study endpoints analyses. SAE denotes serious adverse event.

linked immunosorbent assay (ELISA) or immunofluorescence assay (IFA), respectively (22). On the basis of these data, we assessed antibodies against PfCSP and the entire PfSPZ (IFA) as well as performed a functional assay using subject

serum so as to assess inhibition of sporozoite invasion (ISI) in a hepatocyte line in vitro.

Two weeks after the final vaccination, there was a correlation between the total dosage of PfSPZ Vaccine administered and results of PfCSP

ELISA, PfSPZ IFA, and PfSPZ ISI (Spearman $R = 0.77, 0.83$ and 0.84 , respectively; $P < 0.001$) (Fig. 3, A to C). Among the nine subjects who received four doses of 1.35×10^5 PfSPZ Vaccine, antibodies for all three assays were numerically

Table 1. Frequency of solicited and unsolicited adverse events. Solicited reactogenicity was collected for 7 days after each vaccination. Each vaccine recipient is counted once at worst severity for any local and systemic

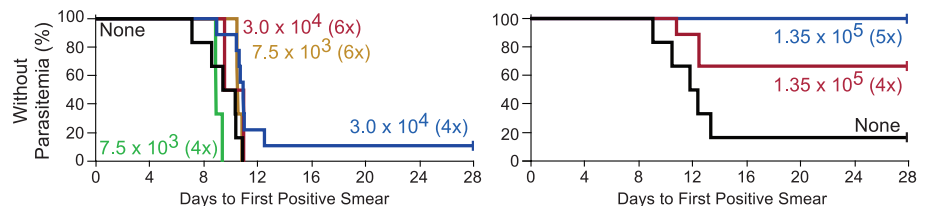
parameter. Unsolicited AE percentages indicate the number of vaccine recipients with the given event (regardless of severity) divided by the total number who received PfSPZ Vaccine.

	$\leq 7.5 \times 10^3$ PfSPZ per dose ($n = 9$ subjects)	3×10^4 PfSPZ per dose ($n = 12$ subjects)	1.35×10^5 PfSPZ per dose ($n = 19$ subjects)	All groups ($n = 40$ subjects)
Number (%)				
Any local reactogenicity				
None	8 (88.9)	10 (83.3)	12 (63.2)	30 (75.0)
Mild	1 (11.1)	1 (8.3)	7 (36.8)	9 (22.5)
Moderate	0 (0)	1 (8.3)	0 (0)	1 (2.5)
Severe	0 (0)	0 (0)	0 (0)	0 (0)
Any systemic reactogenicity				
None	6 (66.7)	7 (58.3)	6 (31.6)	19 (47.5)
Mild	3 (33.3)	4 (33.3)	9 (47.4)	16 (40.0)
Moderate	0 (0)	1 (8.3)	3 (15.8)	4 (10)
Severe	0 (0)	0 (0)	1 (5.3)	1 (2.5)
Unsolicited adverse events*				
Number with one or more adverse event	8 (88.9)	11 (91.7)	17 (89.5)	36 (90)
ALT and/or AST increased	5 (55.6)	6 (50)	5 (26.3)	16 (40)
Upper respiratory tract infection	3 (33.3)	2 (16.7)	5 (26.3)	10 (25.0)
Anemia	2 (22.2)	1 (8.3)	3 (15.8)	6 (15.0)
Leukopenia	2 (22.2)	0 (0)	2 (10.5)	4 (10)
Neutropenia	0 (0)	0 (0)	4 (21.1)	4 (10)
Gastroenteritis	0 (0)	1 (8.3)	3 (15.8)	4 (10)
Eosinophilia	1 (11.1)	1 (8.3)	1 (5.3)	3 (7.5)
Lymphopenia	0 (0)	1 (8.3)	2 (10.5)	3 (7.5)
Thrombocytopenia	0 (0)	2 (16.7)	1 (5.3)	3 (7.5)
Leukocytosis	0 (0)	0 (0)	2 (10.5)	2 (5.0)
Abdominal pain	0 (0)	0 (0)	2 (10.5)	2 (5.0)
Diarrhea	0 (0)	0 (0)	2 (10.5)	2 (5.0)
Dyspepsia	0 (0)	0 (0)	2 (10.5)	2 (5.0)
Muscle strain	0 (0)	1 (8.3)	1 (5.3)	2 (5.0)
Dizziness	0 (0)	1 (8.3)	0 (0)	1 (2.5)
Pruritus	0 (0)	1 (8.3)	0 (0)	1 (2.5)

*MedDRA terms for which one or more AE was assessed as possibly related to vaccination are shown; adverse event terms for which no events were considered related are not shown. Frequency of any hepatic enzyme adverse event [alanine aminotransferase (ALT) increased, aspartate aminotransferase (AST) increase, or both] are counted together; more detail on these events is available in table S4.

Fig. 2. Kaplan-Meier curves and protection table results.

Kaplan-Meier curves are shown for the July and October CHMIs, indicating the frequency of subjects who remained without *Plasmodium falciparum* parasitemia after CHMI. CHMI Parasite* refers to the Pf parasite used to produce infected mosquitoes for CHMI (supplementary materials). Each dose group and regimen is labeled and listed in the tables. Vaccine efficacy (VE) against acquiring *P. falciparum* malaria is shown in the last column. For the groups receiving the 1.35×10^5 dose of PfSPZ Vaccine in the October CHMI, estimates of VE [defined as $1 - \text{Relative Risk (RR)}$], and (exact, unconditional) 95% confidence intervals (CIs) are as follows: five doses, 0/6 versus 5/6 estimated RR = 0; estimated VE = 100% [95% CI for VE (0.464, 1)]; four doses, 3/9 versus 5/6 estimated RR = 0.4; estimated VE = 60% [95% CI for VE (-0.127, 0.92)]; combined, 3/15 versus 5/6 estimated RR = 0.24; estimated VE = 76% [95% CI for VE (0.272, 0.955)].



Vaccination Dose	# Inj.	CHMI Parasite*	# of Subjects	Parasite Free	Vaccine Efficacy
None		NF54	6	0	
7.5×10^3	4	NF54	3	0	0%
7.5×10^3	6	NF54	3	0	0%
3.0×10^4	4	NF54	9	1	11%
3.0×10^4	6	NF54	2	0	0%

Vaccination Dose	# Inj.	CHMI Parasite*	# of Subjects	Parasite Free	Vaccine Efficacy
None		3D7	6	1	
1.35×10^5	4	3D7	9	6	60%
1.35×10^5	5	3D7	6	6	100%

higher in the six protected than the three non-protected subjects and significantly higher for the PfSPZ ISI ($P = 0.05$) (Fig. 3, A to C).

Antibodies to asexual or sexual erythrocytic stage parasites and antigens were undetectable, indicating that the irradiated PfSPZ were attenuated and did not develop beyond the early liver stage.

Cellular Immune Responses

Studies in mice and NHPs show that protective immunity induced with irradiated SPZ requires cellular immunity, and most preclinical data indicate that $CD8^+$ T cells and interferon- γ (IFN- γ) are critical mediators of protection (21, 23–25). $CD4^+$ T cells, $CD3^+ \gamma\delta$ T cells, and natural killer (NK) cells can also play a role in protection (24, 26, 27). Therefore, we used multiparameter flow cytometry to assess the frequency of PfSPZ-specific IFN- γ , interleukin-2 (IL-2), tumor necrosis factor (TNF), or perforin-producing $CD3^+CD4^+$,

$CD3^+CD8^+$, and $CD3^+ \gamma\delta$ T cells and NK cells from cryopreserved peripheral blood mononuclear cells (PBMCs) prior to immunization and 2 weeks after the final immunization (fig. S4). The memory phenotype of PfSPZ-specific cells was assessed on the basis of differential expression of the cell-surface markers, CD45RA and CCR7 (fig. S4, C and G).

PfSPZ-specific memory $CD3^+CD4^+$ T cells from a representative protected subject produced IFN- γ , IL-2, and TNF, whereas PfSPZ-specific memory $CD3^+CD8^+$ T cells produced IFN- γ but little TNF and no IL-2 (Fig. 3D). There was a dose-dependent increase in frequency of PfSPZ-specific $CD3^+CD4^+$ T cells ($P \leq 0.001$) and $CD3^+CD8^+$ T cells producing any combination of IFN- γ , IL-2, or TNF ($P = 0.01$) (Fig. 3E).

We assessed PfSPZ-specific, IFN- γ -producing T cells in subjects who received 1.35×10^5 PfSPZ Vaccine per injection because of the critical role of IFN- γ in mediating attenuated SPZ-induced

protective immunity. For PfSPZ-specific $CD3^+CD4^+$ IFN- γ -producing T cells, there was no significant difference between protected and un-protected subjects (Fig. 4A). For PfSPZ-specific $CD3^+CD8^+$ IFN- γ -producing T cells, protected subjects who received four doses showed a trend toward higher and more consistent responses (Fig. 4A). Although all subjects who received five doses were protected, there was considerable variability in their responses. In terms of memory phenotype, PfSPZ-specific cytokine-producing $CD3^+CD4^+$ T cells were detected in central (T_{CM}) and effector (T_{EM}) memory subsets (Fig. 4B and figs. S4G and S5). In contrast, PfSPZ-specific $CD3^+CD8^+$ T cells were within effector (T_{EM}) and terminal effector (T_{TE}) memory subsets (Fig. 4B and fig. S4G).

We next characterized the quality of PfSPZ-specific T cell cytokine responses. Among PfSPZ-specific $CD3^+CD4^+$ T cells, there were three primary populations, comprising IFN- γ , IL-2, and TNF;

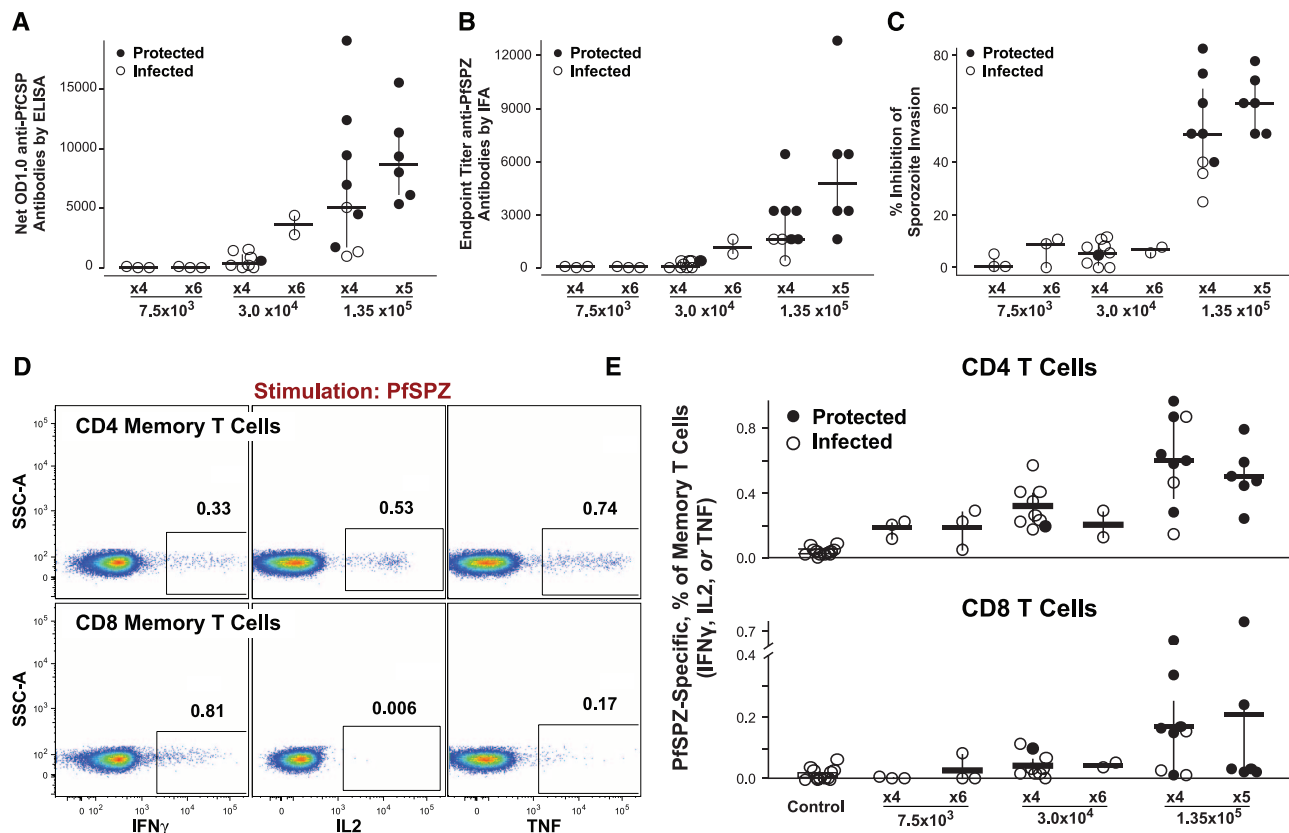


Fig. 3. Antibody, $CD3^+CD4^+$, and $CD3^+CD8^+$ T cell cytokine responses in all immunized participants. (A to C) Antibodies. Assessment of antibodies was performed from serum of all subjects before immunization and 2 weeks after the last dose of the PfSPZ Vaccine, which was ~1 week before CHMI. (A) Net OD 1.0 antibodies to PfCSP by means of ELISA was the serum dilution for each volunteer at which the optical density was 1.0 based on the difference between values in post- and preimmunization serum. (B) Endpoint titer antibodies to PfSPZ by means of IFA for each volunteer was the last serum dilution at which the IFA was positive. (C) Percent inhibition of sporozoite invasion was the percent reduction of the numbers of PfSPZ that invaded a human hepatocyte line in the presence of immune serum as compared with that in the presence of preimmunization serum from the same volunteer, both at a dilution of 1:5. (D and E) T cells. PBMCs were analyzed by means of multiparameter flow

cytometry for PfSPZ-specific cytokine-producing (IFN- γ , IL-2, or TNF) memory $CD3^+CD4^+$ and $CD3^+CD8^+$ T cells from all subjects at week 2 after the final immunization with PfSPZ Vaccine after in vitro restimulation (fig. S4). The frequency of PfSPZ-specific memory $CD3^+CD4^+$ and $CD3^+CD8^+$ T cells was calculated as the fraction of cells making any cytokine in response to PfSPZ minus the response to 1% human serum albumin (diluent). (D) A representative dot plot showing PfSPZ-specific IFN- γ , IL-2, or TNF-producing memory $CD3^+CD4^+$ (top) and $CD3^+CD8^+$ (bottom) T cells from a volunteer who received five doses of 1.35×10^5 PfSPZ Vaccine and was protected. (E) The frequency of total PfSPZ-specific cytokine-producing (IFN- γ , IL-2, or TNF) memory $CD3^+CD4^+$ (top) and $CD3^+CD8^+$ (bottom) T cells from all subjects within each group. Data in all four graphs show a point for each subject. Horizontal bars denote the medians, and whiskers denote the interquartile ranges.

IL-2 and TNF; or TNF (Fig. 4C) and no differences between protected and unprotected subjects. In contrast, among protected subjects ~50 to 80% of the total PfSPZ-specific CD3⁺CD8⁺ T cells produced IFN- γ only, as compared with <30% in unprotected subjects (Fig. 4D). The PfSPZ-specific IFN- γ -producing CD3⁺CD8⁺ T cells uniformly expressed perforin, as did other effector lymphocytes populations, except for CD3⁺CD4⁺ T cells (fig. S4F).

CD3⁺ $\gamma\delta$ T cells from naïve humans respond to malaria antigens after *in vitro* stimulation (28). Accordingly, we also detected IFN- γ in CD3⁺ $\gamma\delta$

T cells from the majority of subjects before immunization in response to PfSPZ stimulation (fig. S4D). Although the proportion of CD3⁺ $\gamma\delta$ T cells producing IFN- γ in response to PfSPZ stimulation did not change after vaccination (fig. S4E), the overall frequency of CD3⁺ $\gamma\delta$ T cells increased in subjects who received 1.35×10^5 PfSPZ Vaccine per dose (Fig. 5).

Last, to assess cellular immunity with a method commonly reported for other malaria vaccine trials, we used enzyme-linked immunosorbent spot assays to enumerate the frequency of IFN- γ responses to PfSPZ and six Pf proteins. PfSPZ-

specific responses ranged from 100 to 300 spot-forming cells (SFCs) per 10^6 PBMCs and were highest in the 1.35×10^5 PfSPZ Vaccine five-dose group (fig. S6A). Responses to stimulation with peptide pools spanning five individual Pf pre-erythrocytic stage antigens were low to undetectable (mostly <100 SFCs per 10^6 PBMCs) but generally higher than to one Pf blood-stage antigen included as a control (MSP1) (fig. S6B).

Discussion

The protection against infection we observed in all of the subjects who received the highest dosage

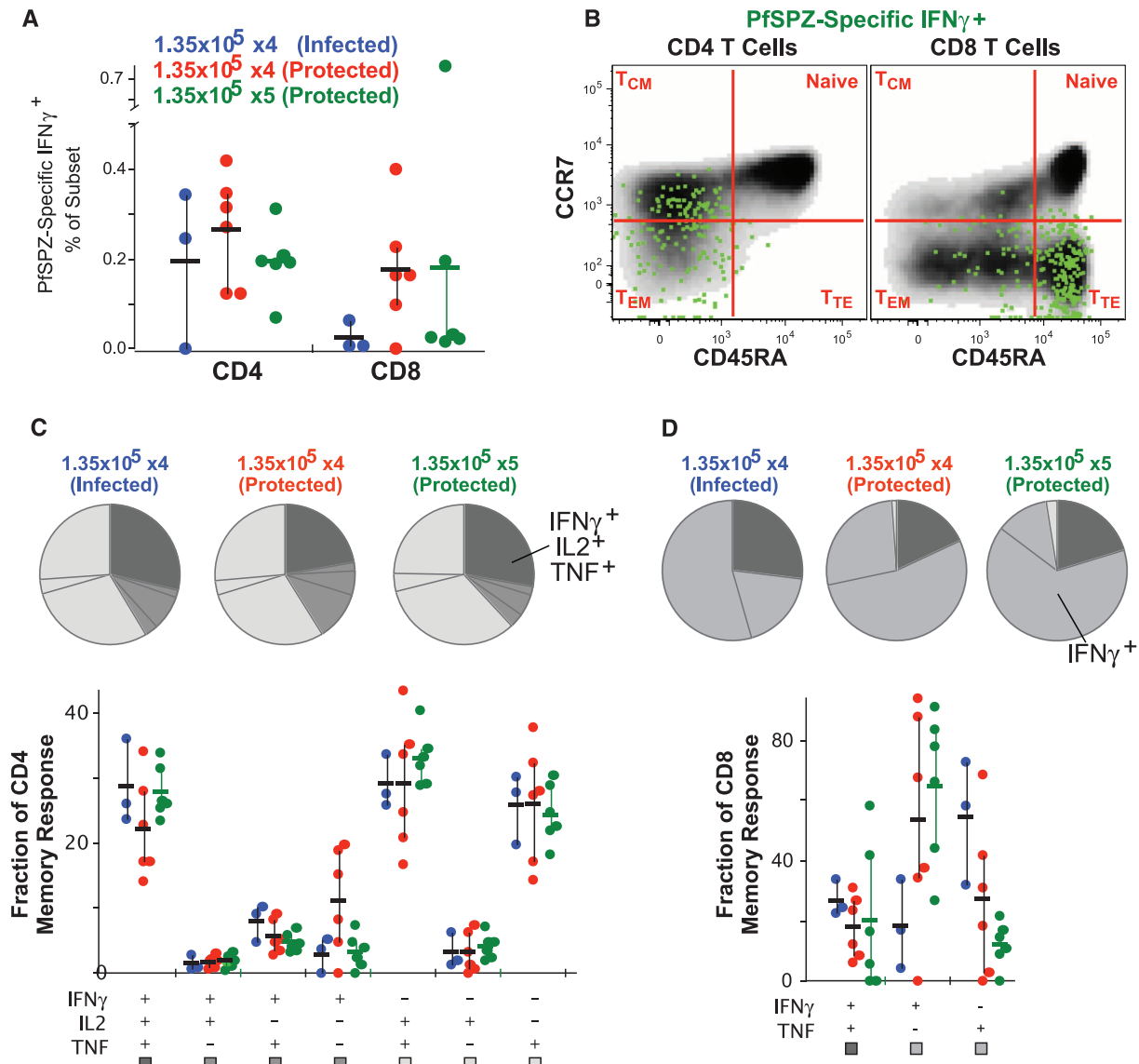
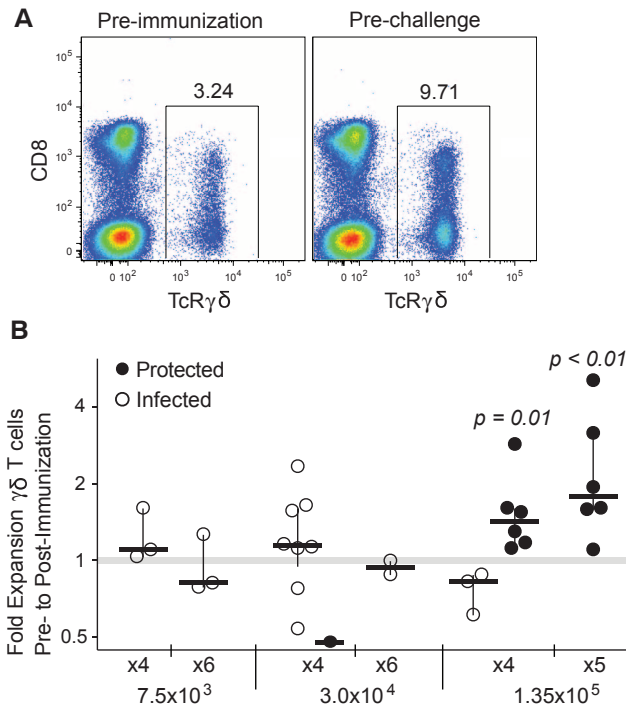


Fig. 4. Magnitude and quality of PfSPZ-specific memory T cell cytokine responses in participants immunized with 1.35×10^5 PfSPZ per dose.

PBMCs were analyzed by means of multiparameter flow cytometry after *in vitro* stimulation with PfSPZ in all volunteers at week 2 after administration of final dose of 1.35×10^5 PfSPZ Vaccine (fig. S4). (A) The frequency of IFN- γ -producing memory CD3⁺CD4⁺ or CD3⁺CD8⁺ T cells in all protected and unprotected subjects who received 1.35×10^5 PfSPZ Vaccine either four or five times. (B) A representative dot plot showing the distribution of PfSPZ-specific IFN- γ -producing CD3⁺CD4 and CD3⁺CD8⁺ T cells within T_{CM}, T_{EM}, and T_{TE} phenotype T cells as defined by expression of CCR7 and CD45RA from a volunteer who

received five doses of 1.35×10^5 PfSPZ Vaccine. The quality of PfSPZ-specific memory (C) CD3⁺CD4⁺ and (D) CD3⁺CD8⁺ T cell response was determined by using Simulation Program with Integrated Circuit Emphasis (SPICE) analysis, defining distinct populations producing any combination of IFN- γ , IL-2, or TNF (CD3⁺CD4⁺) or any combination of IFN- γ or TNF (CD3⁺CD8⁺) at the single-cell level. The relative proportions of each of these populations from the three unprotected and six protected subjects who received four or five doses of 1.35×10^5 PfSPZ Vaccine is shown by pie charts or plotted as a percentage of the total cytokine response. In (A), (C), and (D), a point is shown for each subject. Horizontal bars denote the medians, and whiskers denote the interquartile ranges.

Fig. 5. Expansion of TCR $\gamma\delta$ T cells after immunization with PfSPZ Vaccine. PBMCs were analyzed for frequency of TCR $\gamma\delta$ T cells in all subjects immunized with PfSPZ Vaccine preimmunization and pre-CHMI, as shown in fig. S4. (A) A representative dot plot showing the frequency of TCR $\gamma\delta$ T cells preimmunization and pre-CHMI from a volunteer immunized with five doses of 1.35×10^5 PfSPZ Vaccine. (B) The fold expansion in the total frequency of TCR $\gamma\delta$ T cells after immunization with PfSPZ Vaccine is shown for subjects from all groups and distinguishes protected from nonprotected volunteers. In (B), a point is shown for each subject. Horizontal bars denote the medians, and whiskers denote the interquartile range.



of PfSPZ Vaccine has only been achieved previously through immunization with whole PfSPZ administered through mosquito bites (11, 29). The dose threshold at which we observed the highest rate of protection is consistent with prior studies in which >90% protection was associated with exposure to >1000 irradiated PfSPZ-infected mosquitoes (11).

The five-dose group in which all vaccinees were protected differed in two potentially important ways from other groups. These subjects received the highest total number of PfSPZ Vaccine (6.75×10^5), and there was a 7-week interval between the fourth and fifth doses. We do not know whether the protection in all subjects who received five doses as compared with subjects who received four doses of 1.35×10^5 PfSPZ Vaccine was due to the total dosage of PfSPZ, the numbers of doses, or the increased interval between the fourth and fifth dose. Studies in NHPs show that extending the time between the fourth and fifth dose to ~8 weeks boosted the PfSPZ-specific CD8⁺ T cell responses as compared with that of 4 weeks. Demonstrating that modifications in dose and schedule can achieve a protective immunological threshold in humans will guide future clinical trials designed to optimize the immunization regimen.

Two clinical trials of the PfSPZ Vaccine have established that IV administration of PfSPZ Vaccine induced superior immunogenicity and protective efficacy as compared with those of SC and ID administration (14). The findings are consistent with prior studies in NHP that show IV administration induced a higher frequency of liver resident CD8⁺ T cells specific for PfSPZ and antibodies against PfSPZ (14). Although the IV route is routinely used for therapeutic inter-

ventions in humans, it has not previously been used for administration of preventive vaccines against infectious diseases. Accordingly, a series of clinical trials of the PfSPZ Vaccine administered with IV injection are now planned in Africa, Europe, and the United States to expand critical data on the vaccine for clinical development as a method to prevent malaria in travelers, military, and other high-risk groups and for mass immunization of populations to eliminate Pf malaria from geographically defined areas. The findings of the current study suggest that the protective immune threshold could potentially be achieved in humans with higher numbers of PfSPZ administered in fewer doses by a different schedule or by other routes, as has been done in mice (14). This could be facilitated with microneedle arrays or other novel devices.

The dose-dependent increase in the frequencies of PfSPZ-specific CD3⁺CD4⁺, CD3⁺CD8⁺, and CD3⁺ $\gamma\delta$ T cells in the peripheral blood after immunization is consistent with studies of Pf infection and treatment (28). Because CD3⁺ $\gamma\delta$ T cells and other IFN- γ -producing cells such as NK cells represent a higher proportion of lymphocytes in liver as compared with blood in humans (30), they could contribute to protection.

Although we detected PfSPZ-specific CD3⁺CD8⁺ T cells in 7 of 12 protected subjects at 1.35×10^5 PfSPZ Vaccine per dose, five protected subjects had low to undetectable responses. This finding is consistent with data obtained from NHP studies. We reported that some NHPs with a high frequency (~3%) of PfSPZ-specific CD3⁺CD8⁺ T cells in the liver had no detectable responses in blood after IV immunization with PfSPZ Vaccine (14). We speculate that as in mice (21, 23, 24) and NHPs (25), PfSPZ-specific CD3⁺CD8⁺ T

cells are required for protection in most individuals and are primarily confined to the liver because of persistence of parasite antigens after vaccination and/or retained as tissue-resident memory cells (31).

There was a dose-dependent increase in PfSPZ-specific antibodies using three assays. Although antibodies may have contributed to protection, such responses may best be used to predict vaccine take and serve as a biomarker or nonmechanistic correlate of protection.

Vaccine efficacy against CHMI in this trial was considerably higher than that induced by subunit vaccines (6, 32) and consistent with data generated by immunization with mosquito bites (11). However, the antibody and cellular immune responses induced by the PfSPZ Vaccine against the specific malaria antigens tested were substantially lower than those induced by experimental Pf subunit vaccines (6, 32–35). It remains an open question whether protection results from the summation of multiple low-level antigen-specific responses or from robust responses to a small number of as-yet unidentified antigens from among the ~1000 proteins expressed by sporozoites (36). We show that there are multiple populations of lymphocytes responding to PfSPZ, providing a breadth of effector responses. Furthermore, we speculate that the PfSPZ Vaccine induces immunity to a broad spectrum of antigens among the ~1000 expressed by attenuated PfSPZ (36–38). The capacity to induce a cascade of multiple adaptive and innate effector cells and the breadth of antigenic specificity may explain the advantage of whole PfSPZ vaccines compared with existing subunit vaccines.

Demonstration of high-level protection through IV administration is a critical first step in the development of the PfSPZ Vaccine. Future studies will determine the duration of protection and degree of protection against heterologous strains of Pf, establish immune correlates of protection, and optimize approaches to deliver IV vaccine administration to achieve the coverage in mass administration campaigns needed to eliminate Pf malaria from defined areas.

References and Notes

- World Health Organization, World Malaria Report: 2012 (2012); available at www.who.int/malaria/publications/world_malaria_report_2012/report/en/index.html.
- C. J. Murray *et al.*, *Lancet* **379**, 413–431 (2012).
- C. V. Plowe, P. Alonso, S. L. Hoffman, *J. Infect. Dis.* **200**, 1646–1649 (2009).
- malERA Consultative Group on Vaccines, *PLoS Med.* **8**, e1000398 (2011).
- Malaria Vaccine Technology Roadmap, 2006; available at www.malariavaccine.org/files/Malaria_Vaccine_TRM_Final.pdf.
- K. E. Kester *et al.*, *J. Infect. Dis.* **200**, 337–346 (2009).
- S. T. Agnandji *et al.*, *N. Engl. J. Med.* **367**, 2284–2295 (2012).
- R. S. Nussenzweig, J. P. Vanderberg, H. Most, C. Orton, *Nature* **222**, 488–489 (1969).
- D. F. Clyde, H. Most, V. C. McCarthy, J. P. Vanderberg, *Am. J. Med. Sci.* **266**, 169–177 (1973).
- K. H. Rieckmann, P. E. Carson, R. L. Beaudoin, J. S. Cassells, K. W. Sell, *Trans. R. Soc. Trop. Med. Hyg.* **68**, 258–259 (1974).

11. S. L. Hoffman *et al.*, *J. Infect. Dis.* **185**, 1155–1164 (2002).
12. T. C. Luke, S. L. Hoffman, *J. Exp. Biol.* **206**, 3803–3808 (2003).
13. S. L. Hoffman *et al.*, *Hum. Vaccin.* **6**, 97–106 (2010).
14. J. E. Epstein *et al.*, *Science* **334**, 475–480 (2011).
15. T. Ponnudurai, J. H. Meuwissen, A. D. Leeuwenberg, J. P. Verhave, A. H. Lensen, *Trans. R. Soc. Trop. Med. Hyg.* **76**, 242–250 (1982).
16. S. Chakravarty *et al.*, *Nat. Med.* **13**, 1035–1041 (2007).
17. S. L. Hoffman, D. L. Doolan, *Nat. Med.* **6**, 1218–1219 (2000).
18. Materials and methods are available as supplementary materials on Science Online.
19. P. Potocnjak, N. Yoshida, R. S. Nussenzweig, V. Nussenzweig, *J. Exp. Med.* **151**, 1504–1513 (1980).
20. V. S. Moorthy, W. R. Ballou, *Malar. J.* **8**, 312 (2009).
21. L. Schofield *et al.*, *Nature* **330**, 664–666 (1987).
22. J. E. Egan *et al.*, *Am. J. Trop. Med. Hyg.* **49**, 166–173 (1993).
23. W. R. Weiss, M. Sedegah, R. L. Beaudoin, L. H. Miller, M. F. Good, *Proc. Natl. Acad. Sci. U.S.A.* **85**, 573–576 (1988).
24. D. L. Doolan, S. L. Hoffman, *J. Immunol.* **165**, 1453–1462 (2000).
25. W. R. Weiss, C. G. Jiang, *PLoS ONE* **7**, e31247 (2012).
26. W. R. Weiss, M. Sedegah, J. A. Berzofsky, S. L. Hoffman, *J. Immunol.* **151**, 2690–2698 (1993).
27. M. Tsuji *et al.*, *Proc. Natl. Acad. Sci. U.S.A.* **91**, 345–349 (1994).
28. A. C. Teirlinck *et al.*, *PLoS Pathog.* **7**, e1002389 (2011).
29. M. Roestenberg *et al.*, *N. Engl. J. Med.* **361**, 468–477 (2009).
30. D. G. Doherty, C. O'Farrelly, *Immunol. Rev.* **174**, 5–20 (2000).
31. I. A. Cockburn *et al.*, *PLoS Pathog.* **6**, e1000877 (2010).
32. J. Chuang *et al.*, *PLoS ONE* **8**, e55571 (2013).
33. J. A. Stoute *et al.*, *N. Engl. J. Med.* **336**, 86–91 (1997).
34. K. E. Kester *et al.*, *J. Infect. Dis.* **183**, 640–647 (2001).
35. G. A. O'Hara *et al.*, *J. Infect. Dis.* **205**, 772–781 (2012).
36. L. Florens *et al.*, *Nature* **419**, 520–526 (2002).
37. A. Trieu *et al.*, *Mol. Cell. Proteomics* **10**, M11.007948 (2011).
38. D. L. Doolan *et al.*, *Proc. Natl. Acad. Sci. U.S.A.* **100**, 9952–9957 (2003).

Acknowledgments: The data presented in this manuscript are tabulated in the main figures and the supplementary materials. The clinical trial was funded and supported by the National Institute of Allergy and Infectious Diseases (NIAID) Intramural Research Program. Production and characterization of the vaccine were supported in part by NIAID Small Business Innovation Research grants 4R44AI055229-08, 3R44AI055229-06S1, and 5R44AI058499-05. Preclinical toxicology and biodistribution studies were supported in part by NIAID preclinical service contract N01-AI-40096. Molecular diagnosis was supported by the Howard Hughes Medical Institute. A materials transfer agreement will be required for the use of recombinant PfMSP-1 and PfEBA-175, HC-04 cells, and 2A10 monoclonal antibody. A number of patents on PfSPZ have been issued, allowed, or filed in the United States and internationally. The U.S. patents include S. L. Hoffman *et al.*, U.S. Patent 7,229,627 (2007) (there is a divisional of this patent with claims directed to aseptic adult *Anopheles*-species mosquitoes and aseptic *Plasmodium*-species sporozoites, USSN 11/726,622); S. L. Hoffman *et al.*, U.S. Patent Pub. US2005/0208078 (2005); and B. K. L. Sim, S. L. Hoffman, M. Li, R. E. Stafford, U.S. Patent Pub. U.S. 2010/0183680 (2010). There is also a patent on HC-04 cells [J. Prachumsri *et al.*, U.S. Patent 7015036 (2006)]. The findings and conclusions in this report are those of the authors and do not necessarily reflect the views of the funding agency or collaborators. The views expressed in this article are those of the author and do not necessarily reflect the official policy or position of the Department of the Navy, Department of the Army, Department of Defense, or the U.S. government. This work was supported by work unit number 6000.RADI.F.A0309. The study protocol was approved by the Naval Medical Research Center Institutional Review Board in compliance with all applicable federal regulations governing the protection of human subjects. J.E.E., T.L.R., J.H.R., J.M., and S.A.D. are military service members. This work was prepared as part of their official duties. Title 17 U.S.C. §101 defines a U.S. government work as a work prepared

by a military service member or employee of the U.S. government as part of that person's official duties. The opinions or assertions contained herein are the private views of the authors and are not to be construed as official or as reflecting true views of the Departments of the Army, Navy, or Defense. The authors thank the vaccine trial participants for their contribution and commitment to vaccine research. We acknowledge the contributions of our NIH Clinical Center and NIAID colleagues, especially A. S. Fauci for thoughtful advice and review of the manuscript; J. Stein, J. Pierson, R. Eckes, P. Driscoll, L. Ediger, and the nursing staff of the SNW, SCSU, 5SE-S, and 5SE-N units; our VRC colleagues, especially B. Flynn, A. Mittelman, M. Young, C. Artis, R. Hicks, and T. Abram; the EMMES Corporation; R. Thompson, F. Beams, M. Garley, A. Hoffman, and D. Dolberg of Sanaria for administrative, operations, and legal support and T. Luke for insight and inspiration; the NIAID Institutional Review Board; the NIAID Office of Communications and Government Relations; the NIH Clinical Center Investigational New Drug Pharmacy; and the NIH Clinical Center Patient Recruitment and Public Liaison Office. We appreciate the expert reviews of the Safety Monitoring Committee (A. Durbin, K. Kester, and A. Cross) and the assistance from the U.S. Military Malaria Vaccine Program, the Walter Reed Army Institute of Research Entomology Branch, and the Naval Medical Research Center, especially A. Reyes, Y. Alcorta, G. Banania, C. Fedders, M. Dowler, T. Savransky, D. Patel, C. Brando, and K. Kobylinski.

Supplementary Materials

www.sciencemag.org/content/341/6152/1359/suppl/DC1
Materials and Methods
Supplementary Text
Figs. S1 to S6
Tables S1 to S6
References (39–51)

11 June 2013; accepted 25 July 2013
Published online 8 August 2013;
10.1126/science.1241800

REPORTS

Linear Structures in the Core of the Coma Cluster of Galaxies

J. S. Sanders,^{1,2*} A. C. Fabian,² E. Churazov,^{3,4} A. A. Schekochihin,⁵ A. Simionescu,^{6,7,8} S. A. Walker,² N. Werner^{6,7}

The hot x-ray-emitting plasma in galaxy clusters is predicted to have turbulent motion, which can contribute around 10% of the cluster's central energy density. We report deep Chandra X-ray Observatory observations of the Coma cluster core, showing the presence of quasi-linear high-density arms spanning 150 kiloparsecs, consisting of low-entropy material that was probably stripped from merging subclusters. Two appear to be connected with a subgroup of galaxies at a 650-kiloparsec radius that is merging into the cluster, implying coherence over several hundred million years. Such a long lifetime implies that strong isotropic turbulence and conduction are suppressed in the core, despite the unrelaxed state of the cluster. Magnetic fields are presumably responsible. The structures seen in Coma present insight into the past billion years of subcluster merger activity.

Galaxy clusters are the largest gravitationally bound structures and are dominated by dark matter. They are the latest structures to form in the cosmological hierarchical structure formation scenario. They grow through mergers and by the accretion of matter. Most of their baryonic matter consists of a hot plasma (the intracluster medium, or ICM), heated during cluster formation to temperatures of several 10^7 K and visible by its x-ray emission. Cluster major mergers,

the mergers between clusters of similar mass, are the most energetic events in the local universe, injecting turbulence and motions contributing to the total ICM energy density by around 10% of the thermal value (*1, 2*), increasing with radius.

The Coma cluster of galaxies is one of the best-studied nearby rich clusters. However, it is not dynamically relaxed. X-ray observations have shown the disturbed nature of its ICM (*3, 4*). In particular, a group of galaxies associated with

NGC 4839 to the southwest is merging with the main cluster. Unusually, the cluster has two central giant elliptical galaxies, NGC 4874 and NGC 4889, with a line-of-sight velocity difference of 700 km s^{-1} (*5*). The distribution of galaxy velocities within the cluster implies several different subgroups.

We examined the core of the Coma cluster (Fig. 1) with a 546-ks-deep set of Chandra observations (*6*). At the $\sim 9 \text{ keV}$ (10^8 K) temperature of the ICM in Coma, x-ray surface brightness variations are mainly due to density fluctuations. The most striking features are a set of high-surface-brightness “arms” (labeled A1 to A4). A1 is enhanced in surface brightness with respect

¹Max-Planck-Institut für Extraterrestrische Physik, Giessenbachstrasse 1, 85748 Garching, Germany. ²Institute of Astronomy, University of Cambridge, Madingley Road, Cambridge CB3 0HA, UK. ³Max-Planck-Institut für Astrophysik, Karl-Schwarzschild-Strasse 1, 85748 Garching, Germany. ⁴Space Research Institute (IKI), Profsoyuznaya 84/32, Moscow 117997, Russia. ⁵Rudolf Peierls Centre for Theoretical Physics, University of Oxford, 1 Keble Road, Oxford OX1 3NP, UK. ⁶Kavli Institute for Particle Astrophysics and Cosmology, Stanford University, 452 Lomita Mall, Stanford, CA 94305, USA. ⁷Department of Physics, Stanford University, 382 Via Pueblo Mall, Stanford, CA 94305–4060, USA. ⁸Institute of Space and Astronautical Science, Japan Aerospace Exploration Agency, 3-1-1 Yoshinodai, Chuo-ku, Sagamihara, Kanagawa 252-5210, Japan.

*Corresponding author. E-mail: jsanders@mpe.mpg.de